Modified Maxwell Garnett model for hysteresis in phase change materials

JAMES D FRAME,[1] NICOLAS G GREEN,[1,2] AND XU FANG[1,3]

[1]*School of Electronics and Computer Science, University of Southampton SO17 1BJ, UK*
[2]ng2@ecs.soton.ac.uk
[3]x.fang@soton.ac.uk

Abstract: Analytical modelling of hysteresis is used to provide crucial prediction and insight for phase transitions in materials. Here we present a modified Maxwell Garnett model for analysing electromagnetic hysteresis. The model uses an asymmetric effective medium approximation to describe intermediate states in the phase change, establishing a link between effective medium and hysteresis analysis. Numerical calculation was performed on an example material, vanadium dioxide, for quantitative demonstration and future experimental verification. The model is easy to use, requires very few input parameters, and provides a phenomenological approach to describing electromagnetic hysteresis in various phase change materials.

OCIS codes: (160.4670) Optical materials; (260.2065) Effective medium theory; (310.6860) Thin films, optical properties; (260.2710) Inhomogeneous optical media; (260.3060) Infrared.

References and links

1. M. Wuttig, H. Bhaskaran, and T. Taubner, "Phase-change materials for non-volatile photonic applications," Nat. Photonics **11**, 465-476 (2017).
2. J. S. Meena, S. M. Sze, U. Chand, and T. Y. Tseng, "Overview of emerging nonvolatile memory technologies," Nanoscale Res. Lett. **9**, 526 (2014).
3. Q. H. Zhang, Y. F. Zhang, J. Y. Li, R. Soref, T. Gu, and J. J. Hu, "Broadband nonvolatile photonic switching based on optical phase change materials: beyond the classical figure-of-merit," Opt. Lett. **43**, 94-97 (2018).
4. Y. F. Gao, H. J. Luo, Z. T. Zhang, L. T. Kang, Z. Chen, J. Du, M. Kanehira, and C. X. Cao, "Nanoceramic VO_2 thermochromic smart glass: A review on progress in solution processing," Nano Energy **1**, 221-246 (2012).
5. M. M. Qazilbash, M. Brehm, B. G. Chae, P. C. Ho, G. O. Andreev, B. J. Kim, S. J. Yun, A. V. Balatsky, M. B. Maple, F. Keilmann, H. T. Kim, and D. N. Basov, "Mott transition in VO_2 revealed by infrared spectroscopy and nano-imaging," Science **318**, 1750-1753 (2007).
6. Z. Yang, C. Y. Ko, and S. Ramanathan, "Oxide electronics utilizing ultrafast metal-insulator transitions," Annu. Rev. Mater. Res. **41**, 337-367 (2011).
7. O. Najera, M. Civelli, V. Dobrosavljevic, and M. J. Rozenberg, "Resolving the VO_2 controversy: Mott mechanism dominates the insulator-to-metal transition," Phys. Rev. B **95**, 035113 (2017).
8. M. A. Kats, R. Blanchard, P. Genevet, Z. Yang, M. M. Qazilbash, D. N. Basov, S. Ramanathan, and F. Capasso, "Thermal tuning of mid-infrared plasmonic antenna arrays using a phase change material," Opt. Lett. **38**, 368-370 (2013).
9. Z. H. Zhu, P. G. Evans, R. F. Haglund, and J. G. Valentine, "Dynamically reconfigurable metadevice employing nanostructured phase-change materials," Nano Lett. **17**, 4881-4885 (2017).
10. M. R. M. Hashemi, S. H. Yang, T. Y. Wang, N. Sepulveda, and M. Jarrahi, "Electronically-controlled beam-steering through vanadium dioxide metasurfaces," Sci. Rep. **6**, 35439 (2016).
11. Q. Wang, G. H. Yuan, K. S. Kiang, K. Sun, B. Gholipour, E. T. F. Rogers, K. Huang, S. S. Ang, N. I. Zheludev, and J. H. Teng, "Reconfigurable phase-change photomask for grayscale photolithography," Appl Phys Lett **110**, 201110 (2017).
12. C. Rios, M. Stegmaier, P. Hosseini, D. Wang, T. Scherer, C. D. Wright, H. Bhaskaran, and W. H. P. Pernice, "Integrated all-photonic non-volatile multi-level memory," Nat. Photonics **9**, 725-732 (2015).
13. N. Dávila, Emmanuelle Merced, and Nelson Sepúlveda, "Electronically variable optical attenuator enabled by self-sensing in vanadium dioxide," IEEE Photonics Technol. Lett. **26**, 1011-1014 (2014).
14. A. Visintin, *Differential Models of Hysteresis* (Springer, 1994).
15. I. D. Mayergoyz, *Mathematical Models of Hysteresis and Their Applications* (Academic, 2003).
16. J. Zhang, E. Merced, N. Sepulveda, and X. B. Tan, "Modeling and inverse compensation of hysteresis in vanadium dioxide using an extended generalized Prandtl-Ishlinskii model," Smart Mater. Struct. **23**, 125017 (2014).

17. K. Ito, K. Nishikawa, and H. Iizuka, "Multilevel radiative thermal memory realized by the hysteretic metal-insulator transition of vanadium dioxide," Appl. Phys. Lett. **108**, 053507 (2016).
18. T. C. Choy, *Effective Medium Theory: Principles and Applications* (Oxford University, 2015).
19. H. W. Verleur, A. S. Barker, Jr., and C. N. Berglund, "Optical properties of VO_2 between 0.25 and 5 eV," Phys. Rev. **172**, 788-798 (1968).
20. I. Pirozhenko and A. Lambrecht, "Influence of slab thickness on the Casimir force," Phys. Rev. A **77**, 013811 (2008).
21. M. J. Dicken, K. Aydin, I. M. Pryce, L. A. Sweatlock, E. M. Boyd, S. Walavalkar, J. Ma, and H. A. Atwater, "Frequency tunable near-infrared metamaterials based on VO_2 phase transition," Opt. Express **17**, 18330-18339 (2009).
22. E. D. Palik, *Handbook of Optical Constants of Solids* (Academic, 2012).
23. M. A. Kats, R. Blanchard, S. Y. Zhang, P. Genevet, C. H. Ko, S. Ramanathan, and F. Capasso, "Vanadium dioxide as a natural disordered metamaterial: perfect thermal emission and large broadband negative differential thermal emittance," Phys. Rev. X **3**, 041004 (2013).
24. T. Ung, L. M. Liz-Marzan, and P. Mulvaney, "Optical properties of thin films of Au@SiO_2 particles," J. Phys. Chem. B **105**, 3441-3452 (2001).
25. A. Hatef, N. Zamani, and W. Johnston, "Coherent control of optical absorption and the energy transfer pathway of an infrared quantum dot hybridized with a VO_2 nanoparticle," J. Phys.: Condens. Matter **29**, 155305 (2017).
26. G. Leahu, R. L. Voti, C. Sibilia, and M. Bertolotti, "Anomalous optical switching and thermal hysteresis during semiconductor-metal phase transition of VO_2 films on Si substrate," Appl. Phys. Lett. **103**, 231114 (2013).
27. L. A. L. de Almeida, G. S. Deep, A. M. N. Lima, and H. Neff, "Modeling of the hysteretic metal-insulator transition in a vanadium dioxide infrared detector," Opt. Eng. **41**, 2582-2588 (2002).

1. Introduction

Phase change materials such as chalcogenide glasses and vanadium dioxide (VO_2) can switch between two phases with greatly different properties. This behaviour has provided technological applications including rewritable optical discs, non-volatile electronic memories [1, 2], non-volatile photonic switches [3] and thermochromic smart coatings [4]. The transition between these two phases often involves complicated atomic and electronic changes, the mechanism of which has long been a vibrant topic in condensed matter physics and material sciences [5-7]. More recently, the control of intermediate states in transitions has been explored for developing dynamically tuneable antennae [8, 9], beam steering metasurface [10], grayscale photolithography [11] and multi-level memory [12].

Hysteresis is often evident in phase change materials; in thermally triggered phase change this means different properties upon heating and cooling even at the same temperature. Understanding and modelling hysteretic phase transition is hugely important in device design: For example, in infrared sensors hysteresis is typically avoided but in memory applications, large and controllable hysteresis is integral to their operation [13]. Many analytical models have been developed for hysteresis (e.g. the Preisach model, the Prandtl-Ishlinskii model and the Duhem model) [14, 15]. The choice of model, often with modification, depends on the specific material and/or properties under study [16, 17]. However, while these models are perceived as powerful analytical tools, their usefulness in applications is limited by their complexity.

Here we propose an analytical model for describing electromagnetic hysteresis, which differs from existing models in that it is based on the Maxwell Garnett effective medium approximation. The model is generic and developed for use on arbitrary phase change materials, however, in this paper we will use previous studies on VO_2 for demonstration and validation.

VO_2 shows hysteretic insulator-metal transition close to 68°C. In the low temperature, pure insulator (or semiconductor) phase, it has an infrared complex permittivity of a typical lossy dielectric. Meanwhile, in the high temperature, pure metal phase, the complex permittivity shows characteristics of a metal, with negative real and large imaginary component. The crystalline structure is monoclinic and tetragonal in the insulator and metal phase, respectively. For the intermediate states during the phase transition, these two phases co-exist and form complicated nanostructures [5]. For infrared light with wavelengths above a micrometre, these nanostructures are indiscernible and the whole material is perceived as a

homogeneous medium, very suitable for the application of effective medium models. (By comparison, other macroscopic properties including DC electrical conductivity may highly depend on the intricate features of the nanostructures, posing significant challenges to the application of any effective medium model). Here, we use VO_2 to demonstrate the modified Maxwell Garnett effective medium model and perform quantitative analysis.

2. Modified Maxwell Garnett effective medium model

As an effective medium theory, the Maxwell Garnett model is frequently used to predict the effective complex permittivity ε_{eff} of a composite formed by two constituents ε_1 and ε_2:

$$\varepsilon_{eff} = \varepsilon_2 \frac{\varepsilon_1(1+2f)+\varepsilon_2(2-2f)}{\varepsilon_1(1-f)+\varepsilon_2(2+f)} \tag{1}$$

where f is the volume fraction (or filling factor) of constituent ε_1 (ranging from 0 to 1). This equation is asymmetric with respect to the two constituents, generally producing a different ε_{eff} if ε_1 and f are interchanged with ε_2 and $1-f$. This asymmetry originates from the assumption that constituent ε_1 is the inclusion while constituent ε_2 is the host. For complicated distributions of two constituents, it is often subjective whether a constituent is the inclusion or the host. This uncertainty has been viewed as a flaw of the model, because ε_{eff} should not change with a person's viewpoint [18].

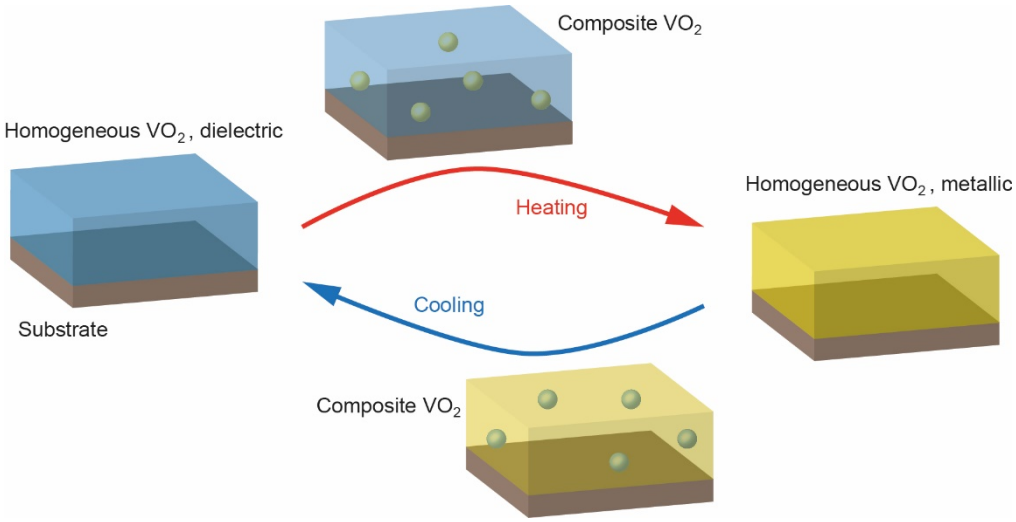

Fig. 1. Viewing hysteresis as an asymmetric structural change. A VO_2 thin film grown on a substrate is used as an example to illustrate the change. The transition between the two homogeneous states shows distinct structural differences in heating and cooling. The embedded spheres approximate the complex, inhomogeneous growth of one pure phase inside another. This view may be adopted for various materials if the modified Maxwell Garnett model is used as a phenomenological approach.

Here we utilise this inherent asymmetry of the Maxwell Garnett model to describe hysteretic phase change. Upon heating, the VO_2 phase transition is generally understood as the nucleation and growth of nanoscale metallic "puddles" within the dielectric matrix [5]. The puddles expand and agglomerate until a continuous metallic film results. Upon cooling, the reverse might be expected to occur, with the metallic puddles shrinking until a continuous

dielectric film results. However, in our model we contend that it instead can be seen as dielectric "islands" growing within the (now) metallic host (Fig. 1). The conventional Maxwell Garnett equation [Eq. (1)] is consequently converted to a pair of equations:

$$\varepsilon_{eff,h} = \varepsilon_d \frac{\varepsilon_m(1+2f)+\varepsilon_d(2-2f)}{\varepsilon_m(1-f)+\varepsilon_d(2+f)} \quad (2)$$

$$\varepsilon_{eff,c} = \varepsilon_m \frac{\varepsilon_m * 2f+\varepsilon_d(3-2f)}{\varepsilon_m(3-f)+\varepsilon_d * f} \quad (3)$$

where the effective permittivity in heating ($\varepsilon_{eff,h}$) and cooling ($\varepsilon_{eff,c}$) is generally different at the same *f*. Unlike the conventional model where f is the volume fraction of the inclusion, our model uses f for a single constituent (here the metallic phase) that can be the inclusion or the host. Both equations describe the pure dielectric phase at $f = 0$ and the pure metallic phase at $f = 1$. At other values of *f*, normally $\varepsilon_{eff,h} \neq \varepsilon_{eff,c}$, with the integral result of hysteresis. Although this modified Maxwell Garnett concept has been mentioned before (e.g. in [18]), we are not aware of another work where it is presented as a positive feature (here used to address hysteretic phase transition).

3. Hysteresis of complex permittivity

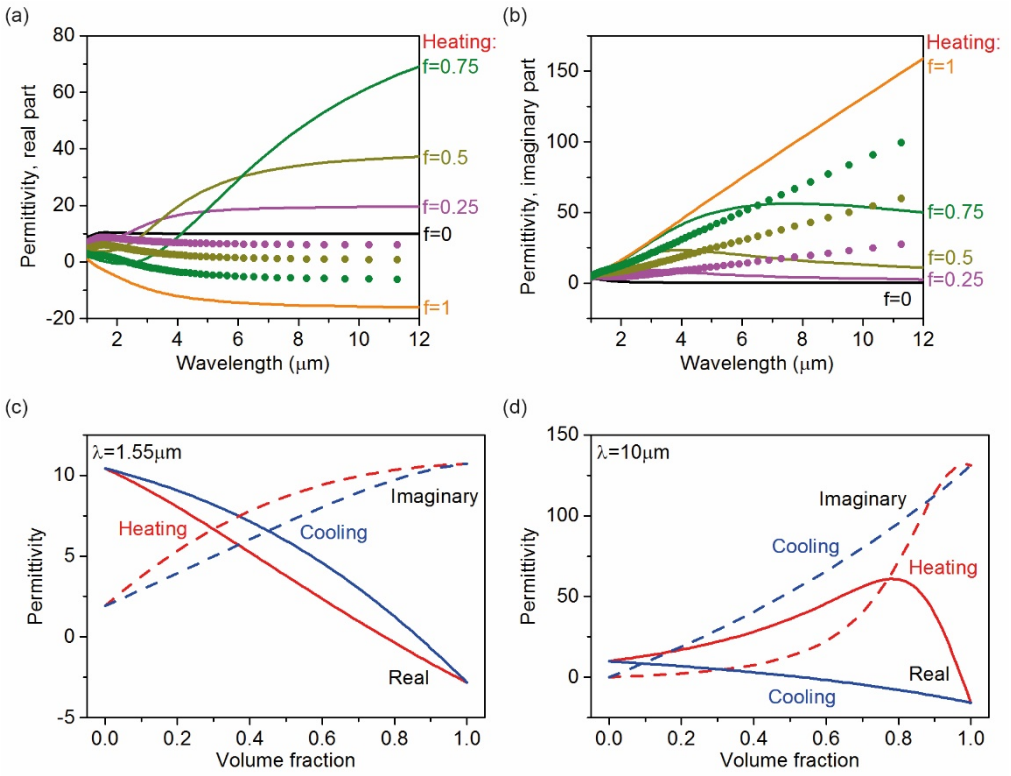

Fig. 2. Complex permittivity of VO_2 calculated based on the modified Maxwell Garnett model. (a) The real part of the permittivity in heating ($\varepsilon_{eff,h}$, lines) and cooling ($\varepsilon_{eff,c}$, dots) with *f* euqals 0 (black), 0.25 (magenta), 0.5 (dark yellow), 0.75 (olive) and 1 (orange). $\varepsilon_{eff,h}$ are labelled for further clarification. $\varepsilon_{eff,h} = \varepsilon_{eff,c}$ at $f = 0$ and $f = 1$. (b) Corresponding imaginary part of the permittivity. (c) $\varepsilon_{eff,h}$ (red) and $\varepsilon_{eff,c}$ (blue) at wavelength 1.55 μm. The

real part is drawn in solid lines, and the imaginary part dashed lines. (d) Corresponding values at 10 μm.

Figure 2 shows the effective permittivity $\varepsilon_{eff,h}$ and $\varepsilon_{eff,c}$ of VO_2 calculated using the modified Maxwell Garnett model. The permittivity of the two pure phases, ε_m and ε_d, is taken from [19, 20]. The model, which originally covers the wavelength range from 0.25 μm to 4.96 μm (i.e. from 0.25 eV to 5.0 eV), is extrapolated here to cover the whole calculated wavelength range following the practice in [21]. Figures 2(a) and 2(b) show the wavelength dependence of the real and imaginary part of the permittivity, respectively, at several representative values of *f*. They reveal that, heating and cooling indeed correspond to very different permittivity. Interestingly, the permittivity during phase transition is not confined by the values of the two pure phases, as observed in Fig. 2(a) for all the calculated intermediate states at long wavelengths.

Figures 2(a) and 2(b) also show that, the phase transition is much more pronounced at long wavelengths than short wavelengths. Figures 2(c) and 2(d) compare 1.55 μm with 10 μm, two example wavelengths at each end of the calculated spectrum range. These two wavelengths are chosen also for technological relevance: 1.55 μm is a standard wavelength for optical fibre communications, and 10 μm is approximately at the centre of the infrared atmospheric window for imaging and sensing. Figures 2(c) and 2(d) show that these two wavelengths share several characteristics: (1) both the real and imaginary part of the permittivity shows hysteresis; (2) at large values of *f*, the real part is negative and the material effectively becomes a metal. Both characteristics agree with common understandings of the material.

The modified Maxwell Garnett model also predicts characteristics at 10 μm that to a certain extent are counter-intuitive. First, a typical hysteresis loop possesses two-fold rotational symmetry. In contrast, both loops in Fig. 2(d) are highly asymmetric and the imaginary part even shows a crossover within the loop. Secondly, a typical hysteresis loop shows the biggest contrast in its output if the input is at the centre of the loop. In contrast, for the real part in Fig. 2(d), the biggest difference between heating and cooling is at $f = 0.8$, very close to an end of the loop. Finally, in a typical hysteresis loop, the output changes monotonically with the input. This general observation is obviously invalid for the real part in heating in Fig. 2(d).

4. Hysteresis of optical reflection

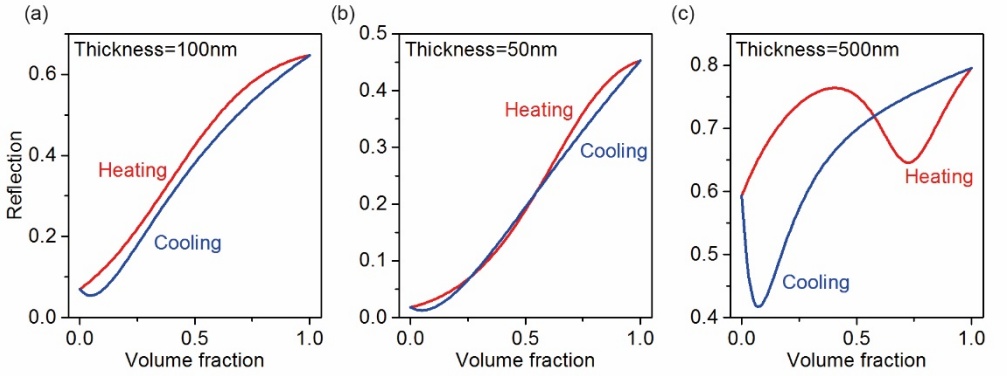

Fig. 3. Reflection of a thin VO_2 film on top of a bulk sapphire substrate. The film thickness is (a) 100 nm, (b) 50 nm, and (c) 500 nm. The light wavelength is 10 μm.

To quantitatively demonstrate our model and to allow for future experimental verification, we analytically calculated optical spectra of three samples using the Fresnel equations. Each sample consists of a thin VO_2 film on top of a bulk sapphire (Al_2O_3) substrate, a substrate that is frequently used to grow VO_2. The wavelength is 10 μm. The permittivity of the two pure phases of VO_2 is $\varepsilon_d = 9.93 + 0.15i$ and $\varepsilon_m = -15.75 + 131.16i$. The complex refractive index of Al_2O_3 is $0.925 + 0.034i$ [22]. As the substrate is slightly absorptive and is assumed to be infinitely thick in the calculation, the transmission is zero. Figure 3 shows the reflection of light from three films with various thicknesses. For a film thickness of 100 nm [Fig. 3(a)], the hysteresis is a single loop roughly possessing two-fold rotational symmetry, a feature commonly seen in various hysteresis loops. This result is interesting as the hysteresis of the permittivity, the only source of the reflection hysteresis, obviously lacks this feature [Fig. 2(d)].

At a smaller thickness of 50 nm [Fig. 3(b)], the hysteresis develops two crossovers, which significantly diminishes the difference between heating and cooling. At a relatively large thickness of 500 nm [Fig. 3(c)], the hysteresis is two pronounced loops connected at $f \approx 0.5$. The reflection covers very different ranges in heating and cooling: its minimal value is 0.59 in the former and 0.42 in the latter. These three example thicknesses in Fig. 3 indicate a rich variety of hysteresis loops observable in experiment. It is worth noting that, the crossover points in Fig. 3 do not imply that $\varepsilon_{eff,h}$ equals $\varepsilon_{eff,c}$. In fact, $\varepsilon_{eff,h} \neq \varepsilon_{eff,c}$ for the whole range of f at 10 μm as seen in Fig. 2(d).

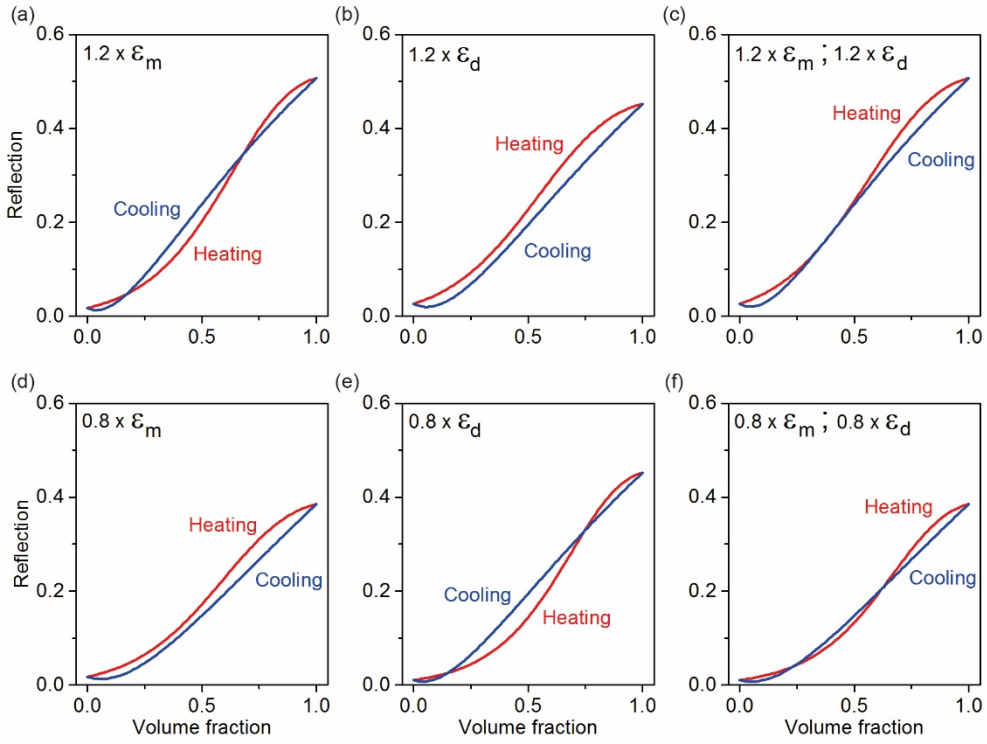

Fig. 4. Dependence of light reflection from a 50 nm thick VO_2 film on the complex permittivity of the material. The permittivity of either one or both of the pure phases is changed by 20% before applying the modified Maxwell Garnett model. From the standard values of ε_m and ε_d, the changes are (a) $1.2 \times \varepsilon_m$, (b) $1.2 \times \varepsilon_d$, (c) $1.2 \times \varepsilon_m$ and $1.2 \times \varepsilon_d$, (d) $0.8 \times \varepsilon_m$, (e) $0.8 \times \varepsilon_d$, and (f) $0.8 \times \varepsilon_m$ and $0.8 \times \varepsilon_d$.

We envisage that the relatively high sensitivity on film thickness shown in Fig. 3 will pose a challenge in future experimental verification of our modified Maxwell Garnett model. An even larger challenge, however, will come from potential discrepancy between the permittivity used here and that of actual samples. In fact, reproducible fabrication of VO_2 thin films with sufficiently high quality has only been established recently, which has triggered great interest in the study of intermediate states [23].

A study of the sensitivity of reflection to the permittivity changes is shown in Fig. (4). In the study one or both of the pure phase permittivity values was changed by 20% before applying the modified Maxwell Garnett model. This change was applied to the metallic phase [Figs. 4(a) and 4(d)], the dielectric phase [Figs. 4(b) and 4(e)], and both phases [Figs. 4(c) and 4(f)]. The film thickness was 50 nm, the same as in Fig. 3(b). The two crossovers in Fig. 3(b), which could serve as a unique marker in experiments, disappear in half of the cases [Figs. 4(b), 4(c) and 4(d)]. This result suggests that the reflection hysteresis can be highly sensitive to the material permittivity in the pure phases. Interestingly, the same analysis performed for a silicon substrate shows only a single crossover at 50 nm film thickness, and this feature is much less susceptible to changes in film permittivity (see Appendix for details).

5. Discussion

Although experiments hold the ultimate test, we can predict the validity of a new theoretical model by examining its assumptions. The original Maxwell Garnett effective medium model has a main assumption of limited interaction between inclusions. For this reason, it is generally believed to be valid only for very dilute samples. In certain circumstances, however, it can accurately predict electromagnetic behaviour up to a volume fraction f of 0.5 [24], and has been adopted in theoretical analysis with f up to 1 [25]. Generally, effective medium theories are most accurate when the two phases have little variation between their complex permittivity. Based on these considerations, the range of validity of the modified Maxwell Garnett model should depend on both the material and the spectral characteristics.

An alternative approach presented in the literature for hysteresis is using the non-hysteretic Eq. (1) but introducing hysteresis to the filling factor f by fitting experimental data. [26] took this approach, where f was assumed to be a free parameter and varied nonlinearly with temperature. This approach has two potential drawbacks. First, the permittivity must be in the same range of values for heating and cooling, and consequently cannot explain experiments if the two curves in an optical hysteresis loop do not overlap in the vertical range, a feature which is, in fact, noticeable in the same reference. In contrast, the modified Maxwell Garnett model allows the permittivity to fall in different ranges while heating and cooling [e.g. Fig. 2(d)]. Secondly, it is debatable whether f should be a free parameter if analytical results are used to provide quantitative support to experiment. Whether f is hysteretic is unknown at the moment, as there has been very few studies on the dependence of f on temperature [27]. On the other hand, the modified Maxwell Garnett model does not require f to be hysteretic with temperature, with the hysteresis arising simply from different nanoscale structures in the material during the heating and cooling processes, a concept which is more straightforward and easier to adopt.

6. Conclusion

We have proposed a new analytical model for describing electromagnetic hysteresis in phase change. The model utilises the inherent asymmetry in the conventional Maxwell Garnett approximation to establish a unique approach to the analysis of hysteresis. Permittivity and reflection of VO_2 thin films were numerically calculated to demonstrate the use of the model.

Both conventional and unconventional hysteresis loops were observed with changing the wavelength and film thickness.

A compelling feature of our model is its simplicity: it requires only the volume fraction and the widely available permittivity of each pure phase. It provides a phenomenological approach to interpreting hysteresis and intermediate states of transition between two solid phases of various materials. It may also provide quantitative predictions for suitable materials and wavelength ranges.

Appendix

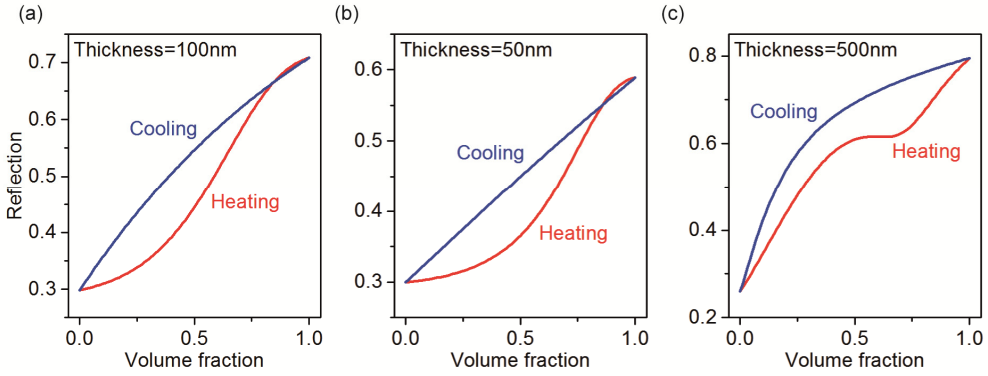

Fig. 5. Reflection of a thin VO_2 film on top of a bulk silicon substrate. The film thickness is (a) 100 nm, (b) 50 nm, and (c) 500 nm. The light wavelength is 10 μm.

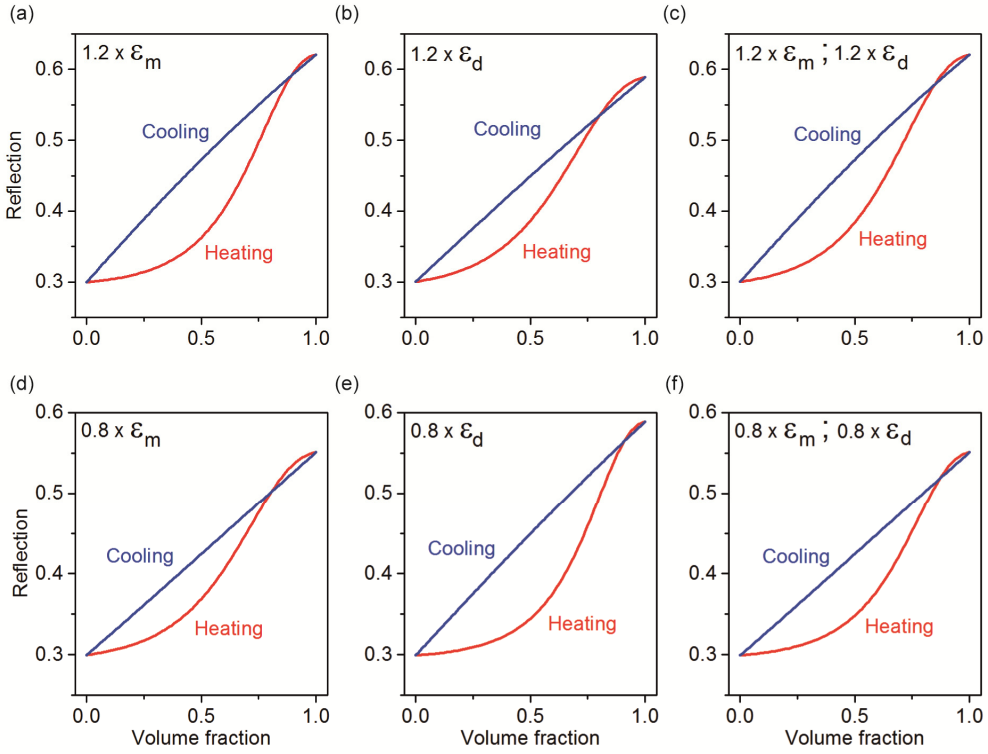

Fig. 6. Data corresponding to Fig. 4 with the Al_2O_3 substrate replaced by Si.

Section 4 demonstrates the influence of the thickness (Fig. 3) and permittivity (Fig. 4) of the VO_2 thin film on the reflection hysteresis. Here we further show the influence of the substrate by replacing the Al_2O_3 substrate with Si, another frequently used substrate material. At the wavelength of interest, 10 μm, Si is lossless with a real refractive index of 3.42. The analytical calculation that produced Figs. 3 and 4 was repeated here to generate Figs. 5 and 6. Figure 5 shows the reflection hysteresis for three different VO_2 thicknessess, 50 nm, 100 nm and 500 nm. A single crossover is observed at 50 nm and 100 nm (Figs. 5(a) and 5(b)), while no crossover exists at 500 nm (Fig. 5(c)). The 50 nm thick film is further analysed in Fig. 6 by changing the permittivity of VO_2 before applying the modified Maxwell Garnett model. The single crossover persists in all the cases.

Funding

The Royal Society (research grant RG170314).